Original Article

Voltammetric sensor for tartrazine determination in soft drinks using poly (*p*-aminobenzenesulfonic acid)/zinc oxide nanoparticles in carbon paste electrode

CrossMark

Ghasem Karim-Nezhad[*], *Zeynab Khorablou, Maryam Zamani,*
Parisa Seyed Dorraji, Mahdieh Alamgholiloo

Department of Chemistry, Payame Noor University, Tehran, Iran

A B S T R A C T

Zinc oxide nanoparticles (ZnO NPs) and *p*-aminobenzenesulfonic acid (*p*-ABSA) were used to fabricate a modified electrode, as a highly sensitive and selective voltammetric sensor, for the determination of tartrazine. A fast and easy method for the fabrication of poly *p*-ABSA (P*p*-ABSA)/ZnO NPs-carbon paste electrode (P*p*-ABSA/ZnO NPs-CPE) by cyclic voltammetry was used. By combining the benefits of P*p*-ABSA, ZnO NPs, and CPE, the resulted modified electrode exhibited outstanding electrocatalytic activity in terms of tartrazine oxidation by giving much higher peak currents than those obtained for the unmodified CPE and also other constructed electrodes. The effects of various experimental parameters on the voltammetric response of tartrazine were investigated. At the optimum conditions, the sensor has a linear response in the concentration range of 0349–5.44 μM, a good detection sensitivity (2.2034 μA/μM), and a detection limit of 80 nM of tartrazine. The proposed electrode was used for the determination of tartrazine in soft drinks with satisfactory results.

1. Introduction

Food additives are commonly used in processed foodstuffs to improve appearance, flavor, taste, color, texture, nutritive value, and preservation. Synthetic colorants, compared with to natural dyestuffs, has been extensively used in food industries in the past four decades because of their higher brightness, more stability, cheapness, and the wider range of shades [1,2].

Generally, synthetic dyes contain azo (N = N) functional groups and aromatic ring structures; therefore, they are harmful to human health [3]. Thus, each synthetic food colorant has been evaluated by the Food and Agricultural Organization and World Health Organization [4]. Tartrazine is one of these azo colorants that may be present in common food products, which can cause allergies, migraines, eczema, anxiety, diarrhea, and even cancer if they are excessively

consumed [5,6]. Facing with increasing legal restrictions, food dye determination has become an analytical challenge. Until now, several methods, such as spectrophotometry [7,8], high performance liquid chromatography (HPLC) [9,10], and capillary electrophoresis [11], have been used for the single or simultaneous determination of tartrazine. On the other hand, electrochemical techniques has obtained much attention and exhibited promising application in food safety analysis due to its portability, excellent sensitivity, automation, short analysis time, low power consumption, and inexpensive equipment [12—18]. Till date, different electrodes have been developed for the single or simultaneous electrochemical determination of different food colorants [19—30].

Carbon electrodes are widely used in electroanalysis due to their low background current, wide potential window, chemical inertness, low cost, and suitability for various sensing and detection applications. Among carbon electrodes, carbon paste electrode (CPE) has a particular importance. The ease and speed of preparation and obtaining a new reproducible surface, very low background current (compared with graphite electrode), low cost, feasibility to incorporate different substances during the paste preparation, and porous surface are some advantages of CPEs over all other carbon electrodes [31]. Therefore, over the past years, CPEs containing various modifiers have been prepared and applied in the determination of different analytes.

The key point to obtain a good and reliable electrochemical sensor is the kind of materials that constitute the detection platform. In this field, the synergy between electrochemical sensors technology and nanomaterials is expecting to bring interesting advantages in the field of new electrochemical transducing platforms beside their use as electrochemical labels or tags for signal enhancement [32]. Sensors based on nanostructured materials take advantages of the increased electrode surface area, increased mass-transport rate, and fast electron transfer compared with electrodes based on bulk materials [32,33]. In addition to novel properties, nanomaterials open up new approaches to fabricate the electrodes cost effectively by minimizing the needed materials and waste generation [34].

Metal oxide nanoparticles have received much attention recently. Various examples of the electrochemical applications are the modification of electrodes with metal oxide nanoparticles in order to develop electrochemical sensors. Among the different metal oxide nanoparticles, zinc oxide (ZnO) is an attractive semiconductor, with a wide band gap (3.37 eV). ZnO has a large excitonic energy, low-cost synthesis, biocompatibility, good electrochemical activities, nontoxicity, high-electron communication features, and high mechanical strength [35]. Nanostructured ZnO has been used previously for the fabrication of different sensors and biosensors [35,36].

On the other hand, polymer-modified electrodes have obtained important attention among the researchers for sensor and biosensor applications because polymeric films have good stability and reproducibility. Electropolymerization is a good method to prepare polymer-modified electrodes as adjusting electrochemical parameters can control film thickness, permeation, and charge transport characteristics.

In this study, we have combined the advantageous features of polymer modification, metal oxide nanoparticles, and carbon paste technology with the aim of electrocatalytic oxidation of tartrazine using poly (p-aminobenzenesulfonic acid) (Pp-ABSA) as a polymer, but with some changes in the carbon paste preparation. The performance of the developed electrode was studied by cyclic voltammetry, and close surface examination was made by scanning electron microscopy (SEM). The fabricated modified electrode facilitated the electron transfer for tartrazine, resulting in the increase of oxidation signals. The performance of the fabricated electrode in tartrazine electroanalysis with respect to sensitivity, selectivity, and linear concentration range was evaluated and discussed. The applicability of the electrode was demonstrated by determining tartrazine in processed soft drinks.

2. Experimental

2.1. Apparatus

Electrochemical measurements were performed on an AUTOLAB modular electrochemical system (ECO Chemie, Utrecht, The Netherlands) equipped with a PGSTAT 12 module and driven by general purpose electrochemical system software (GPES version 4.9) in conjunction with a conventional three-electrode system and a personal computer for data storage and processing. A bare or modified CPE as the working electrode, Ag/AgCl electrode as the reference electrode, and a platinum wire as the auxiliary electrode, were employed in the measurements. SEM images were recorded with KYKY-EM-3200 SEM system (China) at an accelerating voltage of 25 kV.

2.2. Reagents

2.2.1. Chemicals and reagents
Tartrazine was purchased from Aldrich (Canada), and dissolved in water to prepare the standard solution. Desired concentrations were obtained by diluting the standard solution with double distilled water. ZnO nanoparticles (ZnO NPs) were synthesized using solid—vapor phase thermal sublimation techniques. All other chemicals were of analytical grade and used directly. Double distilled water was used throughout the preparation of solutions.

2.2.2. Preparation of modified electrode
First, the ZnO NPs-CPE was prepared by hand mixing 65% graphite powder, 5% ZnO NPs, and 30% paraffin oil in an agate mortar to get a homogeneous carbon paste. Next, the paste was packed in the end of a plastic syringe (2 mm in diameter). A copper wire inserted into the carbon paste provided an electrical contact. The polymer film-modified ZnO NPs-CPE was fabricated by cyclic voltammetry in the potential range −0.6 to +1.8 V at a sweep rate of 100 mV/s in 0.1 M phosphate buffer solution (PBS) pH 7.0 containing 2 mM p-ABSA in the presence of 0.5 M KCl for 15 cycles [37]. The obtained modified electrode (Pp-ABSA/ZnO NPs-CPE) was washed with double distilled water to remove the physically adsorbed material. Stepwise electrodes were also prepared with the same procedures described above for comparison purposes.

3. Results and Discussion

3.1. Characterization of ZnO NPs

Nanoscale ZnO NPs were characterized by SEM and transmission electron microscopy (TEM). Figure 1A shows a typical image of the nanoscale ZnO NPs synthesized via solid–vapor phase thermal sublimation method. It can be observed that it appears to have a rod-like shape with spherical end, with average diameter of 20 nm and length of 10–30 nm, and weak agglomeration can be seen. Figure 1B displays TEM image of nanoscale ZnO NPs. The result shows that the nanoparticles are in the same sizes as shown in the SEM image.

3.2. Surface morphologies of prepared CPEs

SEM technique was utilized to characterize the surface morphologies of the fabricated sensors. The unmodified CPE was characterized by a surface formed by irregularly shaped flakes of graphite that were isolated, and a closer look of the film revealed a broken surface (Figure 2A). SEM images of the separate and consolidated modifiers are also shown (Figures 2B–D). The modification of CPE with P*p*-ABSA and ZnO NPs is clear. The whole assembly on electrode surface (P*p*-ABSA/ZnO NPs-CPE) is shown in Figure 2D. From Figure 2D, it is evident that significant improvement in the surface structure was observed.

3.3. Electrochemical response of modified electrode to Tartrazine

The cyclic voltammograms for different electrodes in the presence of tartrazine at pH 3.0 were investigated in the potential range 0.85–1.200 V versus Ag/AgCl (Figure 3). An irreversible oxidation peak was observed at all four kinds of electrodes, in agreement with previous reports [24]. At the bare CPE (curve a), a weak and broad oxidation peak was observed at about 1.1 V. However, the oxidation current of tartrazine on ZnO NPs-CPE (curve b) and P*p*-ABSA/CPE (curve c) was higher than that of bare CPE, indicating the catalytic activity toward tartrazine oxidation. The step-by-step improvement of peak currents demonstrates the synergistic effect of all two

ingredients of the modified electrode. A significant enhancement in the anodic current (4.8-fold) was achieved at the P*p*-ABSA/ZnO NPs-CPE (curve d) with potential shift, which illustrated that the modified electrode possessed the highest electrocatalytic activity. Increasing the anodic peak current in conjunction with the sharpness of the peak, which is related to a decrease in the overpotential of the process at the surface of the modified electrode, revealed that the modified electrode could act as an effective promoter to enhance the kinetics of the electrochemical process. The results may be ascribed to the high conductivity, good antifouling property, fast electron transfer rate, and high electrochemical activity of the ZnO NPs and P*p*-ABSA. Consequently, the corresponding oxidation peak current of tartrazine on the modified electrode increased greatly.

The differential pulse voltammograms (DPVs) for tartrazine at all four kinds of electrodes were also recorded (Figure 4). As Figure 4 shows, the DPV for 1.49 μM of tartrazine at the unmodified CPE showed a small anodic peak in the potential range 0.85–1.10 V versus Ag/AgCl (Figure 4, curve a). In order to investigate the effect of modifiers on the voltammograms, DPVs for tartrazine at the electrode modified with ZnO NPs and also at the electrode modified with *p*-ABSA were obtained (Figure 4, curves b and c, respectively). As seen in Figure 4 (curves b and c), ZnO NPs increased the surface of the electrode, resulting in an enhancement in the electrochemical properties of the electrode, and the polymer provided a good surface for electron transfer. As a result of synergistic effect from both the above factors, the response of P*p*-ABSA/ZnO NPs-modified CPE increased, and the sensor exhibited excellent electrocatalytic activity and voltammetric performance to the oxidation of tartrazine. This result illustrates that the P*p*-ABSA/ZnO NPs-CPE could present a favorable activity towards the oxidation of tartrazine, suggesting that this electrode will be an excellent sensor for tartrazine determination.

3.4. Optimization of the experimental variables for electrocatalytic oxidation

3.4.1. Effect of amount of ZnO NPs on the electrooxidation of Tartrazine

The effect of the amount of ZnO NPs to be employed as a modifier in the carbon paste was first studied by varying it in
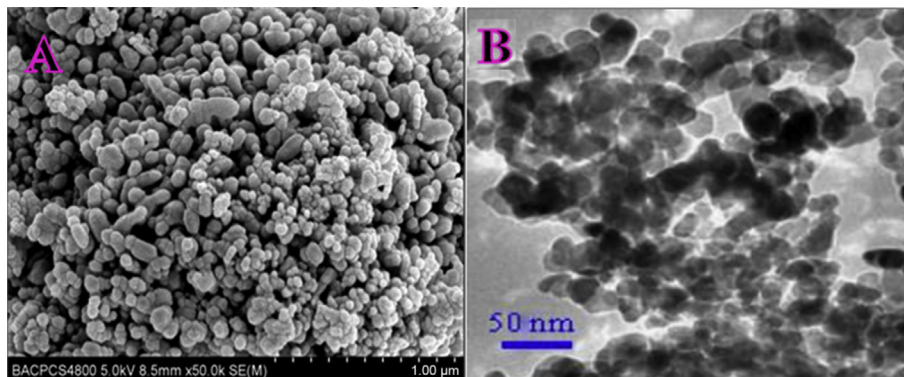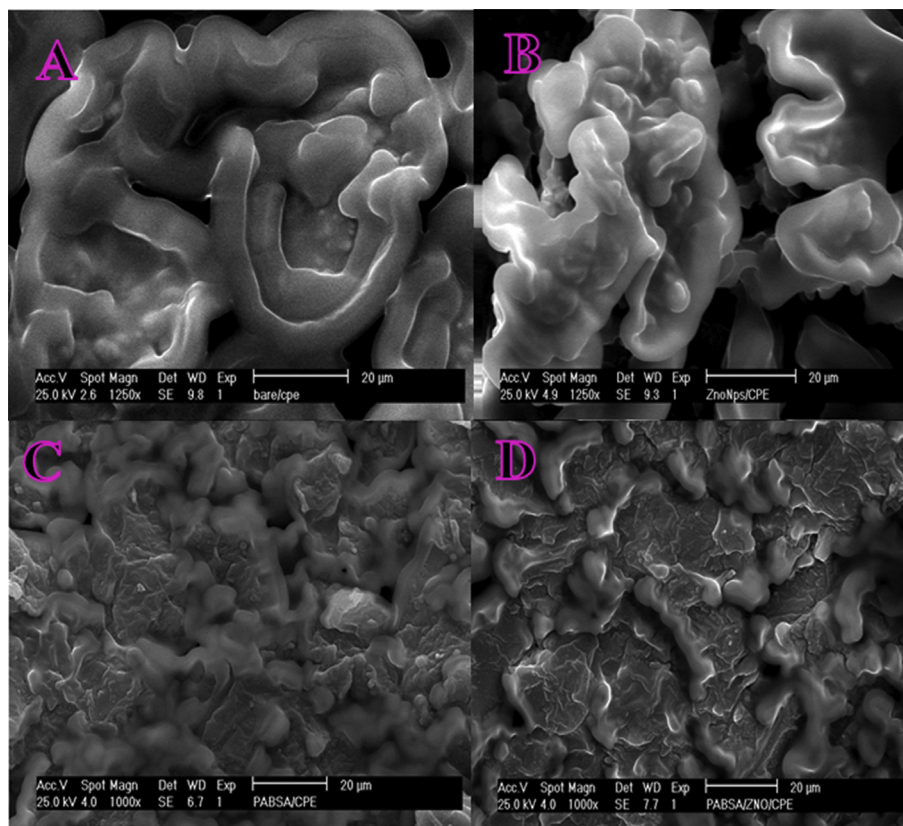

Figure 1 – (A) Scanning electron microscopy image of zinc oxide nanoparticles; (B) transmission electron microscopy image of zinc oxide nanoparticles.

Figure 2 − Scanning electron microscopy images of (A) bare CPE, (B) ZnO NPs-CPE, (C) P*p*-ABSA/CPE, and (D) P*p*-ABSA/ZnO NPs-CPE. CPE = carbon paste electrode; P*p*-ABSA/CPE = poly (*p*-aminobenzenesulfonic acid)/carbon paste electrode; P*p*-ABSA/ZnO NPs-CPE = poly (*p*-aminobenzenesulfonic acid)/zinc oxide nanoparticles carbon paste electrode; ZnO NPs-CPE = zinc oxide nanoparticles carbon paste electrode.

the range of 1−10% with respect to graphite powder. It was observed that the oxidation peak current of tartrazine increased with the increase in percentage up to 5% beyond which saturation in the anodic peak current occurred (Figure 5). As a result, 5% of ZnO NPs was selected as the optimum amount for preparation of P*p*-ABSA/ZnO NPs-CPE.

3.4.2.   *Effect of electropolymerization cycles*
Electropolymerization cycle is another important factor affecting the performance of P*p*-ABSA/ZnO NPs-CPE toward the oxidation current of tartrazine. Figure 6 shows the effect of electro-polymerization cycles on the current response of 5.98 μM tartrazine. The oxidation current increased dramatically with the polymerization cycles increasing from 5 to 15 cycles and decreased after 15 cycles. The reason may be associated with the increase in the thickness of polymeric film resulted in the obstruction of electron transfer on the electrode surface. Therefore, 15 electropolymerization cycles were selected in the following investigation.

3.4.3.   *Influence of supporting electrolyte and solution pH value*
It is well known that the type of supporting electrolyte and the pH value of solution are two important parameters in an electrochemical reaction. Three types of supporting electrolytes, acetate buffer solution, Britton−Robinson buffer

solution, and PBS, have been chosen for use in this study. The results of our tests showed that a more sensitive peak current with respect to tartrazine oxidation was obtained in PBS (data not shown). Thus, PBS was chosen for all the experiments.

The effect of the pH value of solution on the electrochemical oxidation of 6.95 μM tartrazine was also checked in the range of 2.0−9.0 in PBS, as shown in Figure 7. It can be seen that the peak current of tartrazine oxidation is obviously influenced by the pH value. The maximum peak current appeared at pH 3.0. Therefore, pH 3.0 PBS was selected as the optimal buffer pH. As shown in Figure 7, the oxidation peak potential shifted toward less positive with the increase in solution pH, indicating that protons are involved in the oxidation of tartrazine. A good linear relationship between peak potential (E_p) and pH was constructed with the linear regression equation as E_p (V) = −0.0401 pH + 1.2222 (R^2 = 0.9885). The slope value of −0.0401 V/pH was close to the theoretical value of −0.059 V/pH, indicating that an equal number of protons and electrons occurred in electrode reaction.

3.4.4.   *Effect of scan rate*
Performing the voltammograms under different scan rates (Figure 8A) shows that the peak current of the tartrazine oxidation (6.95 μM) is linearly proportional to the square root of the scan rate within the range 20−200 mV/s, suggesting that the tartrazine oxidation follows a diffusion-controlled mechanism (Figure 8B).
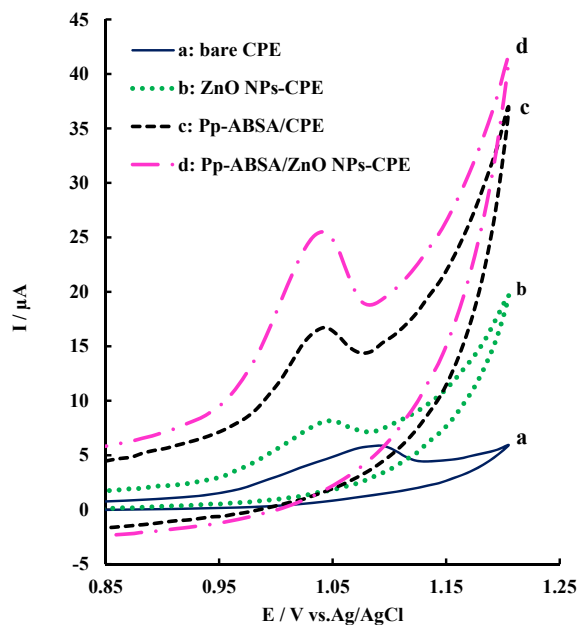
Figure 3 – Cyclic voltammogram responses (I-E) in phosphate buffer solution (PBS; 0.1 M, pH 3.0) and 5.98 μM tartrazine on (a) unmodified CPE, (b) ZnO NPs-CPE, (c) P*p*-ABSA/CPE, and (d) P*p*-ABSA/ZnO NPs-CPE. Scan rate = 100 mV/s. CPE = carbon paste electrode; P*p*-ABSA/CPE = poly (*p*-aminobenzenesulfonic acid)/carbon paste electrode; P*p*-ABSA/ZnO NPs-CPE = poly (*p*-aminobenzenesulfonic acid)/zinc oxide nanoparticles carbon paste electrode; ZnO NPs-CPE = zinc oxide nanoparticles carbon paste electrode.
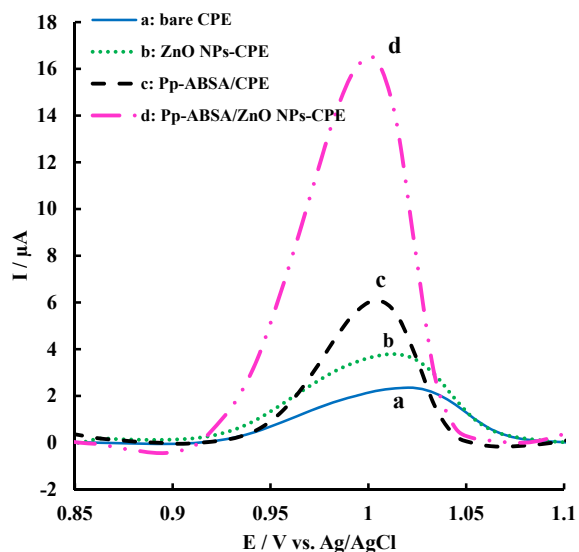
Figure 4 – Differential pulse voltammogram curves (I-E) of 1.49 μM tartrazine on (a) unmodified CPE, (b) ZnO NPs-CPE, (c) P*p*-ABSA/CPE, and (d) P*p*-ABSA/ZnO NPs-CPE. Scan rate = 20 mV/s. CPE = carbon paste electrode; P*p*-ABSA/CPE = poly (*p*-aminobenzenesulfonic acid)/carbon paste electrode; P*p*-ABSA/ZnO NPs-CPE = poly (*p*-aminobenzenesulfonic acid)/zinc oxide nanoparticles carbon paste electrode; ZnO NPs-CPE = zinc oxide nanoparticles carbon paste electrode.
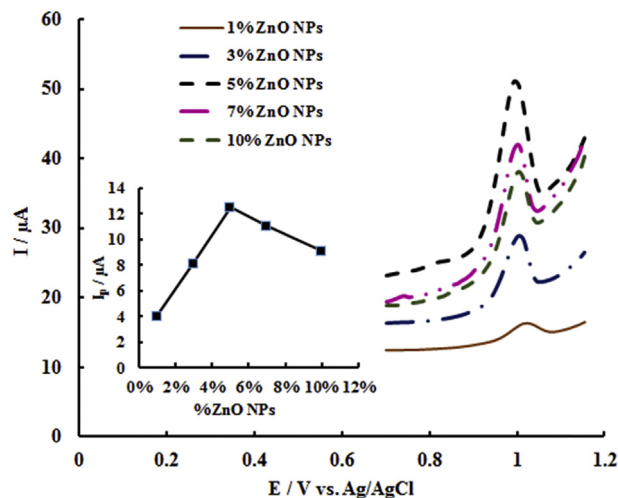

Figure 5 – Differential pulse voltammograms of 5.9 μM tartrazine on the surface of modified electrode with various amounts of zinc oxide nanoparticles (ZnO NPs); (inset) corresponding curve of peak current versus amount of ZnO NPs.

For a diffusion-controlled irreversible anodic reaction, the peak potential, E_p, could be presented by the equation as follows [38]:

$$E_p = b/2 \log (v) + K$$

where v is the scan rate, b is the Tafel slope, and K is a constant value. The plot of E_p versus log (v) was drawn (Figure 8C), and the slope of this plot is 51.5 mV; therefore, the Tafel slope becomes 103 mV/decade. By considering that α equals 0.43, the results indeed suggest one-electron ($n_\alpha = 1.15 \sim = 1$) transfer process in the rate-determining step for the electrocatalytic oxidation of tartrazine.

On the basis of foregoing results in Section 3.4.3 (number of electrons and protons involved in the oxidation of tartrazine were equal), the electrooxidation of tartrazine on P*p*-ABSA/ZnO NPs-CPE was one-electron, one-proton transfer process, in agreement with the previous report [24].
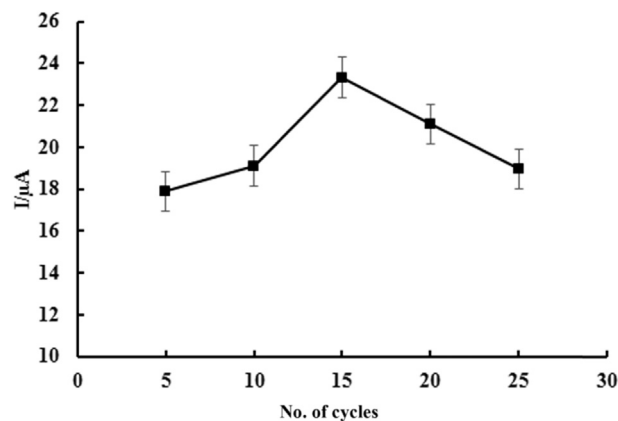
Figure 6 – Curve of peak current versus number of polymerization cycles. Supporting electrolyte is phosphate buffer solution of pH 3.0. Potential scan rate is 100 mV/s.
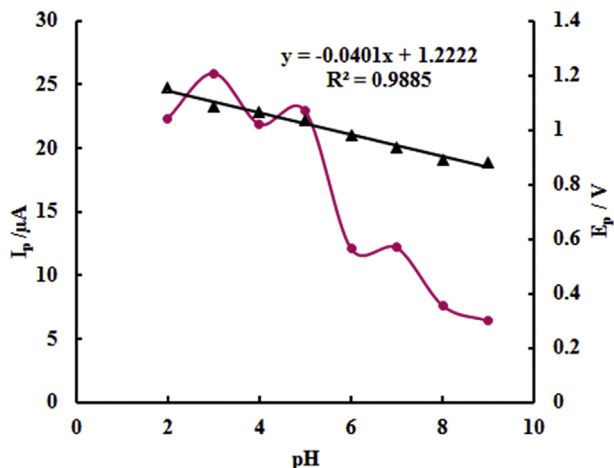
Figure 7 – Plots of peak potential (▲) and peak current (•) against solution pH from cyclic voltammetric study of tartrazine at poly (p-aminobenzenesulfonic acid)/ zinc oxide nanoparticles carbon paste electrode (Pp-ABSA/ZnO NPs-CPE).

3.5. Calibration curve

Under the optimized experimental conditions, the calibration curve for tartrazine at the Pp-ABSA/ZnO NPs-CPE was characterized by differential pulse voltammetry. Figure 9A shows DPVs of various concentrations of tartrazine in phosphate buffer (0.1 M, pH 3.0) on Pp-ABSA/ZnO NPs-CPE. The oxidation peak current of tartrazine increased with increasing concentration of tartrazine. The plot of peak current versus tartrazine concentration had two linear segments corresponding to two concentration ranges of tartrazine (0.0349–1.246 µM and
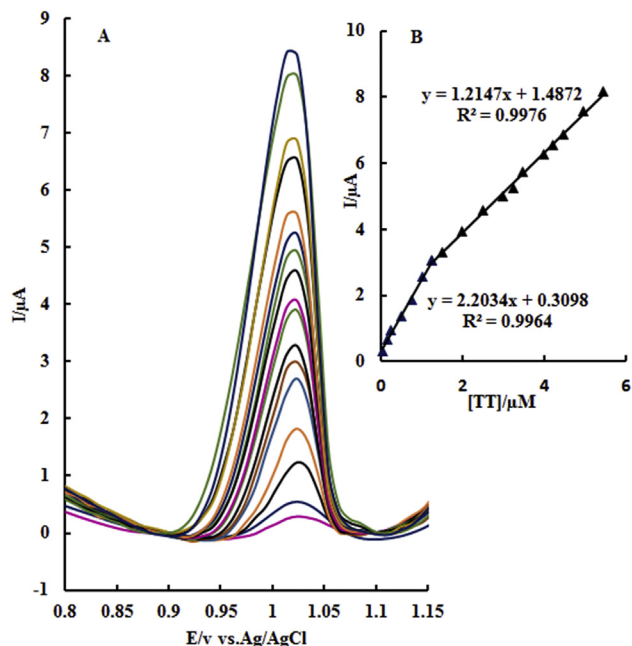

Figure 9 – (A) The differential pulse voltammogram responses of 0.1 M phosphate buffer solution (pH 3.0) with increasing tartrazine concentration on the poly (p-aminobenzensulfonic acid)/zinc oxide nanoparticles carbon paste electrode (Pp-ABSA/ZnO NPs-CPE); (B) the concentration calibration curve for tartrazine (TT).

1.246–5.44 µM), with different slopes (slopes 2.20 for the first and 1.21 for the second linear segments). The decrease of sensitivity (slope) in the second linear range (Figure 9B) was
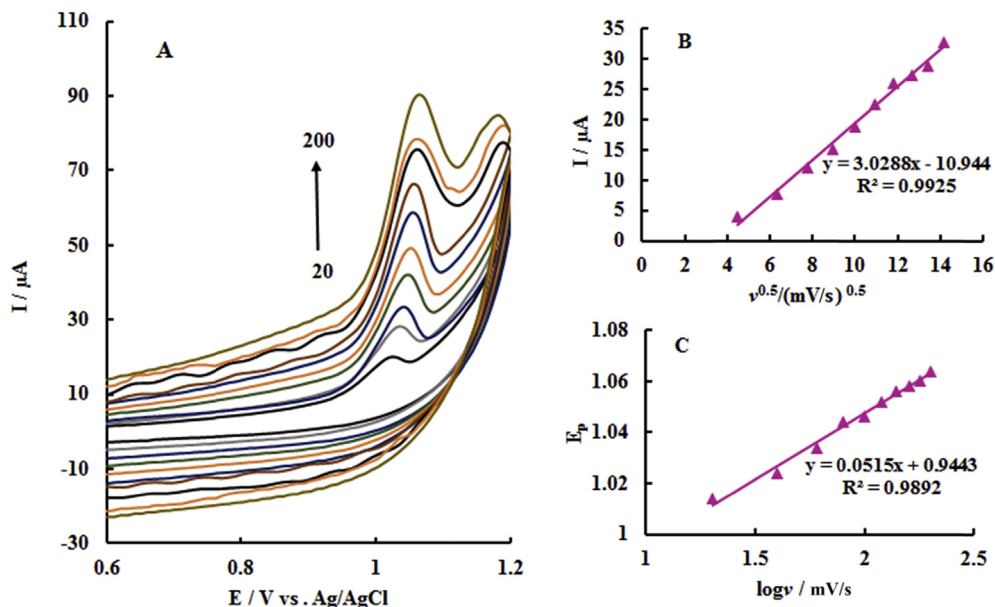
Figure 8 – (A) Cyclic voltammogram responses of 0.1 phosphate buffer solution (pH 3.0) with 6.95 µM tartrazine on the poly (p-aminobenzenesulfonic acid)/zinc oxide nanoparticles carbon paste electrode (Pp-ABSA/ZnO NPs-CPE) at various scan rates (20–200 mV/s); (B) plots of the anodic peak current versus the square root of scan rate ($v^{1/2}$); and (C) relationships between the peak potential and the logarithm of scan rate (log v).

Table 1 – Comparison of the efficiency of some modified electrodes used in the electrocatalysis of tartrazine.

Electrode	Detection limit (nM)	Reference
Gr-TiO$_2$/CPE	8.0	[19]
β-CD-PDDA-Gr/GC-RDE	14.3	[20]
Gr-phosphotungstic acid/GCE	56	[21]
Carbon nanotube/GCE	188	[22]
Acetylene black/GCE	187	[23]
Gold nanoparticles/CPE	2.0	[24]
Alumina microfibers/CPE	2.0	[25]
Gr-Ni nanoparticles/GCE	2.16	[26]
MIP /GCE	1.0	[27]
MWCNTs−IL/CCE	110	[28]
cathodically pretreated boron-doped diamond electrode	62	[29]
MIP-MWNTs-IL@PtNPs/GCE	8.0	[30]
Pp-ABSA/ZnO NPs-CPE	80	This work

Gr-TiO2/CPE = graphene and mesoporous TiO2/carbon paste electrode; β-CD-PDDA-Gr/GC-RDE = β-cyclodextrin coated poly (diallyldimethylammonium chloride)- functionalized graphene/glassy carbon-rotating disk electrode; Gr = graphene; GCE = glassy carbon electrode; CPE = carbon paste electrode; MIP = molecularly imprinted polymer; MWCNT-IL = multiwalled carbon nanotubes-ionic liquid; MIP-MWNTs-IL@PtNPs = molecularly imprinted polymer-multiwalled carbon nanotubes - ionic liquid supported Pt nanoparticles.

likely to be due to kinetic limitations. Limit of detection was calculated as 80 nM ± 0.2 (signal to noise = 3).

The analytical performances of the proposed electrode and other electrodes for the detection of tartrazine are compared and listed in Table 1. Although, a wider linear dynamic and a lower detection limit in most cases was observed ratio to the proposed method. But, the fabricated electrode showed advantages, including high sensitivity, simple modification process, very easy surface update, and good stability. Additionally, the method can be performed using inexpensive equipment in a relatively short time.

3.6. Interference studies

One of the most important problems in practical applications of sensors is the effect of interfering species possibly present in real samples. The influence of various potentially interfering substances with the determination of tartrazine (1.99 μM) was studied under the optimum conditions at pH 3.0 using DPV. The tolerance limit was defined as the maximum concentration of the interfering substance that caused an error of less than ±5% for the determination of tartrazine. It was found that 1000-fold Cu^{2+}, Fe^{2+}, sucrose, glucose, glycine, and ascorbic acid and 50-fold sunset yellow and quinolone yellow had no effect on the detection of tartrazine.

In addition, the results also showed that NH_4^+, Zn^{2+}, Mn^{2+}, Mg^{2+}, Ca^{2+}, Fe^{3+}, Na^+, Cl^-, Zn^{2+}, SO_4^{2-}, K^+, Mg^{2+}, NO_3^- (each for 5.0×10^{-2} M) have no effect on the determination of tartrazine.

From these results, it may be concluded that the method is free from interference by most foreign substances. In view of its inherent selectivity combined with its great operational stability, the proposed sensor shows promising properties for use in real samples with minimal sample preparation.

3.7. Reproducibility and stability of modified electrode

The storage stability and reproducibility of Pp-ABSA/ZnO NPs-CPE were investigated. After 2 weeks storage in dry state at ambient conditions, 94.3% of the initial current signal was retained, indicating that the prepared electrode had acceptable long-term stability.

Five Pp-ABSA/ZnO NPs-CPEs, prepared with the same fabrication procedures, were used for the determination of 1.246 μM tartrazine. The reproducibility, expressed as relative standard deviation (RSD%), was 4.8%. For 10 successive measurements of tartrazine (1.246 μM) with the same electrode, RSD% was 2.55%, which shows good repeatability of the method. The excellent long-term stability and reproducibility of the Pp-ABSA/ZnO NPs-CPEs, make them attractive in the field of analytical applications.

3.8. Real sample analysis

In order to illustrate the application of suggested sensor in real samples analysis, it was employed to detect tartrazine in several processed food stuffs, such as soft drinks and orange powder, produced in Iran. The contents were determined using the standard addition method (Table 2). Five replicate measurements were performed, and satisfactory results were obtained. To test the accuracy of this sensor, the content of tartrazine was also analyzed using HPLC. The results obtained by HPLC and this sensor were in good agreement, revealing that this sensor is satisfactory. In addition, known amounts of

Table 2 – Determination of tartrazine in soft drink samples.

Sample	Pp-ABSA/ZnO NPs-CPE				HPLC		
	Added (μM)	Expected (μM)	Found (μM)	Recovery (%)	Expected (μM)	Found (μM)	Recovery (%)
Orange powder	—		0.045			0.047	
	1	1.045	1.115	106.7	1.047	1.08	103.1
	2	3.045	2.985	98.0	3.047	3.02	99.11
Coolak drink	—		0.053			0.056	
	1	1.053	1.103	104.7	1.056	1.09	103.2
	2	3.053	3.09	101.2	3.056	3.07	100.4

CPE = carbon paste electrode; HPLC = high performance liquid chromatography; NPs = nanoparticles; Pp-ABSA = poly (p-aminobenzenesulfonic acid); ZnO = zinc oxide.

tartrazine were spiked in the samples, and subsequently analyzed according to the same procedure. The value of recovery was higher than 98%, indicating that the fabricated sensor represents a good and easy way for monitoring tartrazine in real samples.

4.   Conclusion

This work demonstrates that new modified CPE fabricated from polymer/ZnO NPs by cyclic voltammetry, which takes only several minutes, can be used for the quantification of tartrazine in different real samples. The construction method was simpler and less time consuming than our previously reported method. By combining the benefits of polymer/ZnO NPs and CPE, the resulted modified electrode exhibited excellent electrocatalytic activity and voltammetric performance to the oxidation of tartrazine. The sensor was characterized by a relatively fast response, long-term and responsive potential stability, and was successfully applied to the selective determination of tartrazine in different real samples.

Conflicts of interest

The authors declare no conflicts of interest. This article does not contain any studies with human participants performed by any of the authors.

Acknowledgments

R E F E R E N C E S

[1] Ashkenazi P, Yarnitzky C, Cais M. Determination of synthetic food colours by means of a novel sample preparation system. Anal Chim Acta 1991;248:289–99.
[2] Silva SLM, Garcia QBS, Lima CFLJ, Barrado E. Voltammetric determination of food colorants using a polyallylamine modified tubular electrode in a multicommutated flow system. Talanta 2007;72:282–8.
[3] López de Alba PL, López Martínez L, Cerdá V, De León Rodríguez LM. Simultaneous determination of tartrazine, sunset yellow and allura red in commercial soft drinks by multivariate spectral analysis. Quim Anal 2001;20:63–72.
[4] Nevado JJB, Cabanillas CG, Salcedo AMC. Method development and validation for the simultaneous determination of dyes in foodstuffs by capillary zone electrophoresis. Anal Chim Acta 1999;378:63–71.
[5] Rowe KS, Rowe KJ. Synthetic food coloring and behavior: a dose response effect in a double-blind, placebo-controlled, repeated-measures study. J Pediatr 1994;125:691–8.
[6] Stevenson DD, Simon RA, Lumry WR, Mathison DA. Adverse reactions to tartrazine. J Allergy Clin Immunol 1986;78:182–91.

[7] Aktas AH, Ertokus GP. Spectral simultaneous determination of tartrazine, allura red, sunset yellow and caramel in drink sample by chemometric method. Rev Anal Chem 2010;29:107–15.
[8] Coelho TM, Vidotti EC, Rollemberg MC, Medina AN, Baesso ML, Cella N, Bento AC. Photoacoustic spectroscopy as a tool for determination of food dyes: comparison with first derivative spectrophotometry. Talanta 2010;81:202–7.
[9] Culzoni MJ, Schenone AV, Llamas NE, Garrido M, Di Nezio MS, Band BSF, Goicoechea HC. Fast chromatographic method for the determination of dyes in beverages by using high performance liquid chromatography—diode array detection data and second order algorithms. J Chromatogr A 2009;1216:7063–70.
[10] Yoshioka N, Ichihashi K. Determination of 40 synthetic food colors in drinks and candies by high-performance liquid chromatography using a short column with photodiode array detection. Talanta 2008;74:1408–13.
[11] Lee KS, Shiddiky MJA, Park SH, Park DS, Shim YB. Electrophoretic analysis of food dyes using a miniaturized microfluidic system. Electrophoresis 2008;29:1910–7.
[12] Goyal RN, Gupta VK, Bachheti N. Fullerene-C60-modified electrode as a sensitive voltammetric sensor for detection of nandrolone—an anabolic steroid used in doping. Anal Chim Acta 2007;597:82–9.
[13] Goyal RN, Gupta VK, Chatterjee S. Voltammetric biosensors for the determination of paracetamol at carbon nanotube modified pyrolytic graphite electrode. Sens Actuators B 2010;149:252–8.
[14] Gupta VK, Goyal RN, Sharma RA. Anion recognition using newly synthesized hydrogen bonding disubstituted phenylhydrazone-based receptors: poly(vinyl chloride)-based sensor for acetate. Talanta 2008;76:859–64.
[15] Gupta VK, Karimi-Maleh H, Sadegh R. Simultaneous determination of hydroxylamine, phenol and sulfite in water and waste water samples using a voltammetric nanosensor. Int J Electrochem Sci 2015;10:303–16.
[16] Jain R, Gupta VK, Jadon N, Radhapyari K. Voltammetric determination of cefixime in pharmaceuticals and biological fluids. Anal Biochem 2010;407:79–88.
[17] Farahi A, Achak M, El Gaini L, El Mhammedi MA, Bakasse M. Electrochemical determination of paraquat in citric fruit based on electrodeposition of silver particles onto carbon paste electrode. J Food Drug Anal 2015;23:463–71.
[18] Nasirizadeh N, Shekari Z, Nazari A, Tabatabaee M. Fabrication of a novel electrochemical sensor for determination of hydrogen peroxide in different fruit juice samples. J Food Drug Anal 2016;24:72–82.
[19] Gan T, Sun J, Meng W, Song L, Zhang Y. Electrochemical sensor based on graphene and mesoporous TiO$_2$ for the simultaneous determination of trace colourants in food. Food Chem 2013;141:3731–7.
[20] Ye X, Du Y, Lu D, Wang C. Fabrication of β-cyclodextrin-coated poly (diallyldimethylammonium chloride)-functionalized graphene composite film modified glassy carbon-rotating disk electrode and its application for simultaneous electrochemical determination colorants of sunset yellow and tartrazine. Anal Chim Acta 2013;779:22–34.
[21] Gan T, Sun J, Cao S, Gao F, Zhang Y, Yang Y. One-step electrochemical approach for the preparation of graphene wrapped-phosphotungstic acid hybrid and its application for simultaneous determination of sunset yellow and tartrazine. Electrochim Acta 2012;74:151–7.
[22] Zhang W, Liu T, Zheng X, Huang W, Wan C. Surface-enhanced oxidation and detection of sunset yellow and tartrazine using multi-walled carbon nanotubes film-modified electrode. Colloids Surf B 2009;74:28–31.

[23] Yang X, Qin H, Gao M, Zhang H. Simultaneous detection of Ponceat 4R and tartrazine in food using adsorptive stripping voltammetry on an acetylene black nanoparticle-modified electrode. J Sci Food Agric 2011;91:2821–5.

[24] Ghoreishi SM, Behpour M, Golestaneh M. Simultaneous determination of sunset yellow and tartrazine in soft drinks using gold nanoparticles carbon paste electrode. Food Chem 2012;132:637–41.

[25] Zhang Y, Hu L, Liu X, Liu B, Wu K. Highly-sensitive and rapid detection of ponceau 4R and tartrazine in drinks using alumina microfibers-based electrochemical sensor. Food Chem 2015;166:352–7.

[26] Gan T, Sun J, Wu Q, Jing Q, Yu Sh. Graphene decorated with nickel nanoparticles as a sensitive substrate for simultaneous determination of sunset yellow and tartrazine in food samples. Electroanalysis 2013;6:1505–12.

[27] Jiang S, Xu J, Xu P, Liu L, Chen Y, Qiao C, Yang S, Sha Z, Zhang J. A novel molecularly imprinted sensor for direct tartrazine detection. Anal Lett 2014;47:323–30.

[28] Majidi MR, Fadakar Bajeh Baj R, Naseri A. Carbon nanotube–ionic liquid (CNT–IL) nanocamposite modified sol-gel derived carbon-ceramic electrode for simultaneous determination of sunset yellow and tartrazine in food samples. Food Anal Method 2012;6:1388–97.

[29] Medeiros RA, Lourencao BC, Rocha-Filho RC, Fatibello-Filho O. Simultaneous voltammetric determination of synthetic colorants in food using a cathodically pretreated boron-doped diamond electrode. Talanta 2012;97:291–7.

[30] Zhao L, Zeng B, Zhao F. Electrochemical determination of tartrazine using a molecularly imprinted polymer –

[31] Svancara I, Schachl K. Testing of unmodified carbon paste. Chem Listy 1999;93:490–9.

[32] Acta Aragay G, Merkoci A. Nanomaterials application in electrochemical detection of heavy metals. Electrochim 2012;49:61–84.

[33] Bagheri H, Afkhami A, Shirzadmehr A, Khoshsafar H, Khoshsafar H, Ghaedi H. Novel potentiometric sensor for the determination of Cd^{2+} based on a new nano-composite. Inter J Envir Anal Chem 2013;93:578–91.

[34] Campbell FW, Compton RG. The use of nanoparticles in electroanalysis: an updated review. Anal Bioanal Chem 2010;396:241–59.

[35] Kumar SA, Chen SM. Nanostructured zinc oxide particles in chemically modified electrodes for biosensor applications. Anal Lett 2008;41:141–58.

[36] Ameen S, Akhtar MS, Seo HK, Shin HS. ZnO quantum dots engrafted graphene oxide thin film electrode for low level detection of ethyl acetate. Mater Lett 2014;136:379–83.

[37] Lin X, Kang G, Lu L. DNA/Poly(p-aminobenzensulfonic acid) composite bi-layer modified glassy carbon electrode for determination of dopamine and uric acid under coexistence of ascorbic acid. Bioelectrochemistry 2007;70:235–44.

[38] Bard AJ, Faulkner LR. Electrochemical methods: fundamentals and applications. 2nd ed. New York: John Wiley & Sons; 2001.

multiwalled carbon nanotubes – ionic liquid supported Pt nanoparticles composite film coated electrode. Electrochim Acta 2014;146:611–7.